

VISUAL TRACKING ON THE GROUND

A Comparative Analysis

Jorge Raul Gomez, Jose J. Guerrero and Elias Herrero-Jaraba

Aragon Institute for Engineering Research, University of Zaragoza, Maria de Luna 1, Zaragoza, Spain

Keywords: Tracking on the ground, Kalman filter, Homography.

Abstract: Tracking is an important field in visual surveillance systems. Trackers have been applied traditionally in the image, but a new concept of tracking has been used gradually, applying the tracking on the ground map of the surrounding area. The purpose of this article is to compare both alternatives and prove that this new usage makes possible to obtain a higher performance and a minimization of the projective effects. Moreover, it provides the concept of *multi-camera* as a new tool for mobile object tracking in surveillance scenes, because a common reference system can be defined without increasing complexity. An automatic camera re-calibration procedure is also proposed, which avoids some practical limitations of the approach.

1 INTRODUCTION

Real-time object tracking is recently becoming more and more important in the field of video analysis and processing. Applications like traffic control, user-computer interaction, on-line video processing and production and video surveillance need reliable and economically affordable video tracking tools. In the last years this topic has received an increasing attention by researchers. However, many of the key problems are still unsolved. The surveillance tracking community in particular has studied target tracking techniques for a number of years, mainly in the context of finding efficient methods to track missiles, aircrafts etc. and tracking targets of unknown motion. Their work has been used for a variety of applications.

There have been previous contributions in order to improve such systems. Tissainayagam and Suter (Tissainayagam and Suter, 2001) proposed a tracking method in which a model switching was used. Other authors, as Isler (Isler et al., 2005), use the technique of multiple or distributed sensors, assigning sensors to track targets so as to minimize the expected error in the resulting estimation for target locations. In most of the cases, the sensors used for these tasks are inherently limited, and individually incapable of estimating the target state, and they only can be used for a unique task. This limitation disappears with the use of cameras. In this way, Lee et al. (Lee et al., 2000) suggested to establish a common coordinate frame and to

capture image signals from several cameras arranged in a particular environment. This last idea is used in this paper in order to demonstrate that this solution contributes a better solution to the tracking problem.

We propose a simple tracker based on the Kalman Filter. This tracker is used in two different ways (on the image plane and on the ground plane), making a comparative between both. Theoretically, the perspective effects must disappear in the second one, and therefore, the tracking must involve better. This paper shows this event such in laboratory conditions as in real environments.

This paper is organized as follows: Section 2 briefly details the transformation between the image and the ground. After that an automatic re-calibration procedure that avoids some of the practical limitations of the approach is proposed. Section 3 provides details of the tracking on the floor, showing the different stages of the proposed tracking system: detection, tracking, uncertainty transformation, and tuning. In Section 4 we provide our results in a particular environment (our laboratory) under stable conditions. Finally, some results for a more complex environment (a football match) are shown also in section 4.

2 FROM IMAGE TO THE GROUND

In order to transform the coordinates from the image to the planar ground, a plane projection transformation is used. At the moment no distortion of the camera lens is assumed. A point in the projective plane is represented by three coordinates, $\mathbf{p} = (x_1, x_2, x_3)^T$, which represents a ray through the origin in the 3D space (Mundy and Zisserman, 1992). Only the direction of the ray is relevant, so all points written as $\lambda\mathbf{p} = (\lambda x_1, \lambda x_2, \lambda x_3)^T$ are equivalent. The classical Cartesian coordinates of the point (x, y) can be obtained intersecting the ray with a special plane perpendicular to x_3 axis and located at unit distance along x_3 . This is equivalent to scale \mathbf{p} as, $\mathbf{p} = (x, y, 1)^T$. Projected points in an image and real points in a planar ground are both represented in this way.

A projective transformation between two projective planes (1 and 2) can be represented by a linear transformation $\mathbf{p}_2 = \mathbf{T}_{21}\mathbf{p}_1$. If the transformation is represented in Cartesian coordinates it results non-linear. Since points and lines are dual in the projective plane, the transformation for the line coordinates is also linear, being $(\mathbf{T}_{21}^{-1})^T$ the corresponding transformation matrix for lines.

2.1 Computing the Transformation to Calibrate the Camera

Let it be $\mathbf{p}_c = (x_i, y_i, 1)^T$ the coordinates of a point i in the camera reference system. Let it be (x_i^g, y_i^g) the coordinates of the corresponding point in a reference system of the planar ground obtained from the plane of the building, and therefore let it be $\mathbf{p}_g = (x_i^g, y_i^g, 1)$ its homogeneous coordinates.

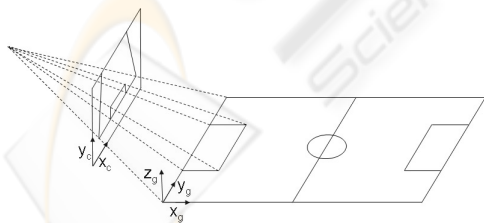


Figure 1: Diagram depicting the transformation of coordinates from image to the ground.

We obtain the projective transformation \mathbf{T}_{gc} up to a non-zero scale factor, for points, $\mathbf{p}_g = \mathbf{T}_{gc}\mathbf{p}_c$. For each couple i of corresponding points, two homogeneous equations to compute the projective transformation are considered. They can be written as, $(\lambda_i x_i^g, \lambda_i y_i^g, \lambda_i)^T = \mathbf{T}_{gc}(x_i, y_i, 1)^T$. Developing them in

function of the elements of the homography matrix, we have

$$\begin{pmatrix} x_i & y_i & 1 & 0 & 0 & 0 & -x_i^g & -y_i^g & -1 \\ 0 & 0 & 0 & x_i & y_i & 1 & -x_i^g & -y_i^g & -1 \end{pmatrix} \mathbf{t} = \begin{pmatrix} 0 \\ 0 \end{pmatrix}$$

where $\mathbf{t} = (t_{11} t_{12} t_{13} t_{21} t_{22} t_{23} t_{31} t_{32} t_{33})^T$ is a vector with the elements of the homography matrix \mathbf{T}_{gc} .

Using four pairs of corresponding points (no three of them being collinear), we can construct a 8×9 matrix \mathbf{M} , where $\mathbf{M}\mathbf{t} = \mathbf{0}$. Then, the solution \mathbf{t} corresponds with the eigenvector associated to the least eigenvalue (in this case the null eigenvalue) of the matrix $\mathbf{M}^T \mathbf{M}$, which can be easily solved by singular value decomposition (svd) of matrix \mathbf{M} . In order to have a reliable transformation, more than the minimum number of point correspondences must be considered, solving in a similar way (Hartley and Zisserman, 2000).

It is known that a previous normalization of data is suitable to avoid numerical computation problems (Hartley, 1997). We have transformed the coordinates of the points (in the image and in the ground) before the computation of the homography to reference systems located in the centroid of the points and scaled in such that the maximum distance of the points to its centroid is 1. After computation of the homography, it is inversely transformed by simple matrix computation to express the homography in the desired reference systems.

2.2 Automatic Camera Re-calibration

Once we have calibrated the camera using at least 4 pairs of corresponding points in the image and in the ground, it cannot be moved, which is the main limitation of this proposal. In practice, due for example to the flexibility of the camera support, the orientation of the camera changes. A little change of orientation has a great influence in the image coordinates of a point, and therefore invalidates previous calibration. However if the camera is not changed in position, or position change is small with respect to the depth of the observed scene, the homography can be re-calibrated automatically with high robustness and without 3D computations. As camera position changes suppose main reconfiguration of the surveillance system, but orientation changes are usual, the automatic re-calibration procedure presented below eliminates the limitation in practice. Besides that, this re-calibration procedure can also be used for changes in zoom lens or motions in pan-tilt cameras demanded by the user.

The re-calibration can be made using features extracted in the image like points and/or lines. We propose to do it using lines because they are plentiful in

man made environments and have other advantages. The straight lines have a simple mathematical representation, they can be extracted more accurately than points being also easier to match them and they can be used in cases where there are partial occlusions.

After extracting the lines, automatic computation of correspondences and homographies is carried out, as previously presented in (Guerrero and Sagüés, 2003), which uses robust estimation techniques. Thus, initially the extracted lines are matched to the weighted nearest neighbor using brightness-based and geometric-based image parameters.

With the coordinates of at least four pairs of corresponding lines we can obtain an homography that transforms both images. As usually we have many more than four line correspondences, an estimation method can be used to process all of them, getting better results. The least squares method assumes that all the measures can be interpreted with the same model, which makes it to be very sensitive to wrong correspondences. The solution is to use robust estimation techniques which detect the outliers in the computation. From the existing robust estimation methods, we have chosen the least median of squares method (Rousseeuw and Leroy, 1987).

In figure 2 we can see an example of two images before and after an unexpected camera motion. The automatic robust matching of lines that allows to compute the camera re-calibration has been superimposed to the images. The initial matching has about 20% of wrong correspondences, but the robust computation of the homography allows to reject wrong matches and also to search more matches according to it in a subsequent step. From the line correspondences the homography to recalibrate the camera is accurately obtained.

3 TRACKING ON THE GROUND

3.1 Detection and Tracking

A widely used technique for separating moving objects from their backgrounds is based on background subtraction (Herrero et al., 2003). In this approach, an image $I_B(x, y)$ of the background is stored before the introduction of a foreground object. Then, given an image $I(x, y)$ from a sequence, feature detection of moving objects are restricted to areas of $I(x, y)$ where:

$$|I(x, y) - I_B(x, y)| > \sigma \quad (1)$$

where σ is a suitable chosen noise threshold.

But this approach exhibits poor results in most real image sequences due to four main problems:

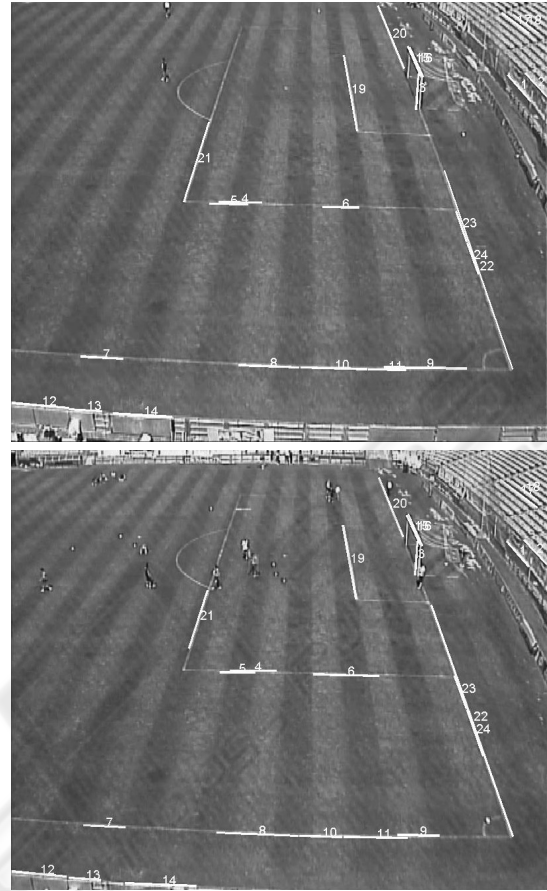


Figure 2: Two images of a football match before and after an unexpected camera motion in a real application. The automatic robust line correspondences has been superimposed to the images.

- Noise in the image.
- Gray level similarity between background and moving objects, even if the color is different.
- Continuous or quick illumination changes in the scene.
- Variation of the static objects in the background.

These problems can be partially solved by an appropriate selection of the threshold value. Some authors (Durucan and Ebrahimi, 2001) (Fabrice Moscheni and Kunt, 1998) have proposed a region-based motion segmentation using adaptive thresholding, according to illumination changes. In addition to this, morphological filters have to be used to eliminate noisy pixels and to fill the moving regions poorly segmented. However, in spite of these improvements, the results that can be found in real situations are far away from a satisfactory solution.

To detect the moving objects, we present an ap-

proach in motion detection, based on difference, introducing two procedures, *Neighborhood-Based Detection* and *Overlapping-Based Labelling*, in order to obtain a more robust segmentation in real scenes. The first one uses a local convolution mask, instead of a punctual one, to compute difference and obtain a more reliable difference image. The second one uses an overlapping criterion between two difference image to classify blobs in two different types: static or dynamic. This last characteristic makes a distinction between moving objects and shadows or illumination changes.

After the motion detection, a Kalman tracker (Kalman, 1960) with a constant velocity model (Bar-Shalom and Fortmann, 1988) is used for tracking, using the center of each detected object as measure data. Internally, the tracker has a state with 4 elements: 2 for the position and 2 for the velocity.

The Kalman filter is divided in two main parts: prediction and estimation. Between them, a matching procedure associates the measures obtained in the motion detection with the prediction of the tracking. It select the nearest-neighbor if it is close enough in function of the covariance of the innovation.

3.2 Uncertainty Transformation

The measure in the Kalman tracker is the position (x, y) of the mobile object. The measure noise has pixel units, but in order to do the tracking in the ground, it must be transformed according to the homography to metric units. To transform the covariance matrix from image to ground, as proposed in (A. Criminisi and Zisserman, 1997), a transformation in three steps is required: change to homogeneous coordinates, transformation of coordinates from image to ground and transformation to inhomogeneous coordinates again.

Given a covariance matrix, which express the uncertainty location in image coordinates:

$$\Lambda_{\mathbf{x}_c}^{2 \times 2} = \begin{pmatrix} \sigma_x^2 & \sigma_{xy} \\ \sigma_{xy} & \sigma_y^2 \end{pmatrix} \quad (2)$$

the correspondent homogeneous one is obtained:

$$\Lambda_{\mathbf{x}_c} = \begin{pmatrix} \Lambda_{\mathbf{x}_c}^{2 \times 2} & \mathbf{0} \\ \mathbf{0}^\top & 0 \end{pmatrix} \quad (3)$$

The change of homogeneous coordinates from image to the ground is made with the homography matrix \mathbf{T}_{gc} . Therefore, the covariance matrix is transformed as:

$$\Lambda_{\mathbf{x}_g} = \mathbf{T}_{gc} \Lambda_{\mathbf{x}_c} \mathbf{T}_{gc}^\top \quad (4)$$

Once we have the uncertainty in the ground in homogeneous coordinates, we need to transform to non-

homogeneous coordinates in order to have the measurement. We will use ∇f as a first-order approximation of the relationship between homogeneous and inhomogeneous coordinates. If $\mathbf{X}_g = (X, Y, W)^\top$

$$\nabla f = 1/W^2 \begin{pmatrix} W & 0 & -X \\ 0 & W & -Y \end{pmatrix} \quad (5)$$

Therefore, the covariance matrix of the measurements noise in ground coordinates is

$$\Lambda_{\mathbf{x}_g}^{2 \times 2} = \nabla f \Lambda_{\mathbf{x}_c} \nabla f^\top \quad (6)$$

This transformation allows to have a noise model which considers the influence of the perspective effect when we made the tracking in the ground.

3.3 Tuning in Practice

The constant velocity model only can be considered locally valid. In practice, there are velocity changes that we model in the process noise. If we consider that the goal have an acceleration which is modelled as a white noise with zero mean and covariance q_i , the state noise matrix \mathbf{Q}_i for each coordinate $i = x_g, y_g$ is (Bar-Shalom and Fortmann, 1988):

$$\mathbf{Q}_i = q_i \cdot \begin{bmatrix} \frac{dt^4}{4} & \frac{dt^3}{2} \\ \frac{dt^3}{2} & dt^2 \end{bmatrix} \quad (7)$$

where dt is the time interval.

If we consider the tracker in the ground, the tuning has a well known meaning, because $\sqrt{q_i}$ represents directly the acceleration of the mobile. On the other hand, the classical tracker in the image needs an empirical tuning in pixel units, that depends of the perspective effect.

The *measure noise matrix* \mathbf{R} is defined in the image for both trackers and transformed to the ground using the homography matrix for the tracker on the ground, as seen in section 3.2.

4 EXPERIMENTS

4.1 Description

The objective of these experiments is to compare the performance of a tracker on the ground versus a tracker on the image. Two Kalman trackers will be compared, using the same constant velocity model, although each one may have a different, but equivalent, tuning, since coordinates in the image and coordinates in the ground represent different magnitudes.

The three first tests performed compare the precision of the predictions of both trackers in a sequence

of 550 frames, recorded with a still camera located in a corridor at 2.5 meters high. The target is a remote-controlled car moving at nearly constant velocity through a corridor, as it can be seen in fig. 3.

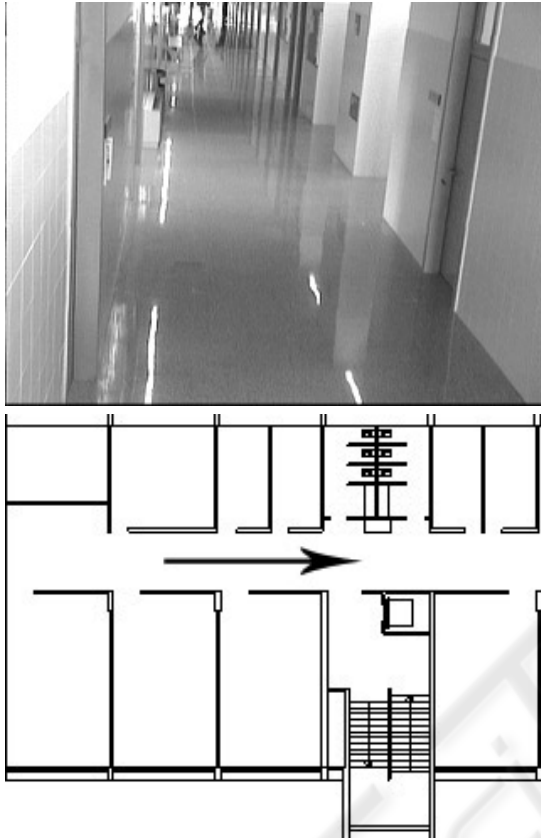


Figure 3: First image of the sequence (up) and building plane (down) where the tests have been performed. The remote-controlled car moves along the corridor in the tests, as the arrow shows.

After obtaining the position of the car in each frame, a tracker on the image has been applied. At the same time, the homography previously calculated, allows us to obtain the corresponding points in the ground for each point in the image, making possible to track the same object with another independent similar tracker on the ground.

To compare the performance of these two trackers, the mean difference between the prediction points and their corresponding measures has been computed. This difference is only taken into account if the measure is considered to belong to the object being tracked. Predictions from these two trackers are going to be compared at three levels: short, medium and long-term.

4.2 Comparative Analysis

Test 1: The first test compares the precision of short-term predictions. In the original sequence, the object is moving away the camera, with occasional lateral movements. The sequence will be tested also in reverse mode, starting from the last frame to the first, making the target go towards the camera. Mean distances obtained between prediction and measures, denoted as d_{pm} , are shown in table 1. All distances are measured in the ground, using Euclidean distance.

Table 1: Mean distances in mm. between predictions and measures for the image tracker and the ground tracker with the sequence processed forwards and backwards.

| d_{pm} | Image | Ground |
|-----------|-------|--------|
| Forwards | 54,90 | 18,89 |
| Backwards | 44,02 | 20,01 |

In this first test, a tracking on the ground has a great advantage over a tracking on the image, since the effect of the perspective deformation is avoided. Distances between predictions and measures are represented in figure 4.

As it can be seen in figure 4, a tracker on the ground obtains better results if the moving object is near the camera, because the velocity of the object in the image is more changeable. However, a tracker on the image obtains opposite results, since only measure noise causes this error. In any case, even when the moving object is far from the camera, the tracker on the ground obtains better results.

It must be noticed that two kinds of source of noise could be considered in the measure: one generated in the detection and other caused by the errors in the homography. At the moment, this second noise source has not been modelled, considering that its effect is small, because all the trajectories are inside the points used to compute the homography matrix in the calibration phase.

Test 2: To compare the accuracy of medium-term predictions, another test will be carried out, in the same sequence, consisting in decimating the number of measures. After the decimation, we will have $550/f$ measures, where f is the decimation factor. The same values for \mathbf{Q} and \mathbf{R} are used. Mean distance d_{pm} will be used again to measure the precision in each case. Obtained results can be seen in table 2, also in mm.

Mean distances grow as decimation factor increases, since the movement of the object is not totally predictable. The tracker on the image has an extra error originated by the deviation in velocity produced by the perspective effect.

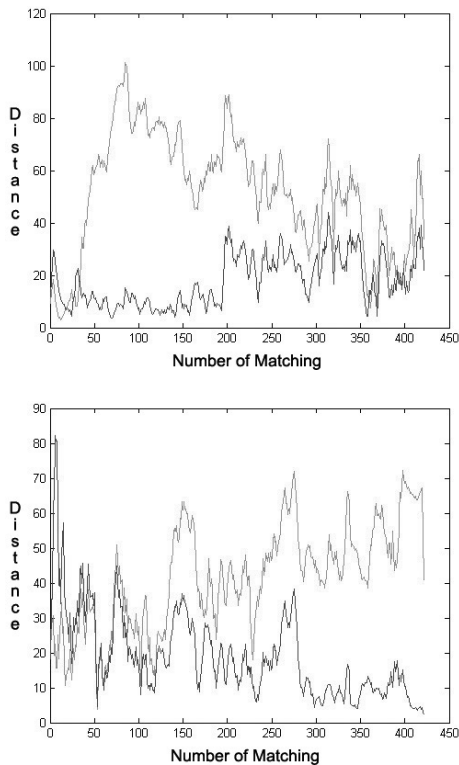


Figure 4: Distance between prediction and measure with tracking on the ground (dark line) and tracking on the image (light line). (a) Target moving away the camera (b) Target moving to the camera.

Table 2: Mean distances in mm. between prediction and measure applying different grades of decimation.

| f | Image | Ground |
|-----|--------|--------|
| 1 | 54,9 | 18,89 |
| 2 | 78,49 | 22,89 |
| 3 | 97,75 | 26,58 |
| 5 | 132,01 | 31,06 |
| 8 | 180,02 | 40,33 |
| 12 | 248,08 | 55,93 |

Test 3: To test the precision of long-time predictions, a determined number of consecutive measures will be erased for both trackers. Also the same values of \mathbf{Q} and \mathbf{R} are used. This test evaluates the possibility of recovering the object after an occlusion.

Different numbers of measures have been erased in each test, from 2 to 100. To measure the accuracy of each tracker, the distance in the ground between the measure and the prediction after the erased block of measures has been used. The results can be seen in figure 5.

Here the differences between both trackers are higher. The ground tracker does not lost the measure

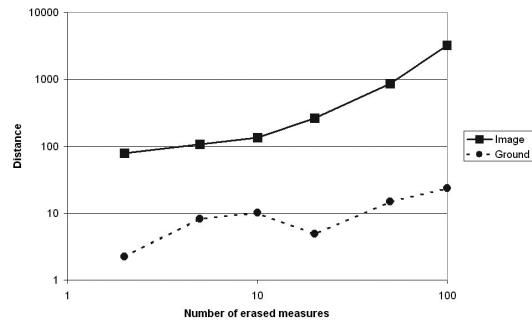


Figure 5: Distances obtained after erased blocks of measures of different lengths (in logarithmic scale).

even after an occlusion of about 100 frames, maintaining short distances between prediction and measure. However, the image tracker easily lost the measure after an occlusion of about 10 frames, giving very bad predictions.

4.3 Using in Practice

Once tested the superiority of the ground tracker in the laboratory, it has been confirmed in real-life videos of a football match. The test consists of a video sequence, as the frame in figure 6.a, where two football players are going to be tracked. Both players are running in parallel trajectories, but at different distances from the camera. In this test, the necessity of re-tuning of each trackers when trying to track different objects will be evaluated.

Both trackers will be configured with different equivalent tunings for the distant player. Using the homography, we can determine the relationship between a pixel in the image and the scale of the field to tune both trackers in a equivalent way. The measure noise \mathbf{R} is fixed, defined for the image tracker, and translated using the homography matrix for the ground tracker. This tuning will be used on the nearby player to check its validity.

The results can be seen on figure 7. As the two trajectories are not equivalent, and may have different accelerations and noises, the results cannot be directly compared. In any case, the figure shows that the number of matchings obtained for the distant player is similar for the two trackers, while the ground tracker obtains more matchings than the image tracker for the nearby player using the same tuning.

Although the number of matchings always can be increased with higher values of the the matrices \mathbf{R} and \mathbf{Q} , the prediction error and the possibility of crossing with other measures would increase as well. Hence, the application for a ground tracker is more important if multiple objects are attempted to be tracked.

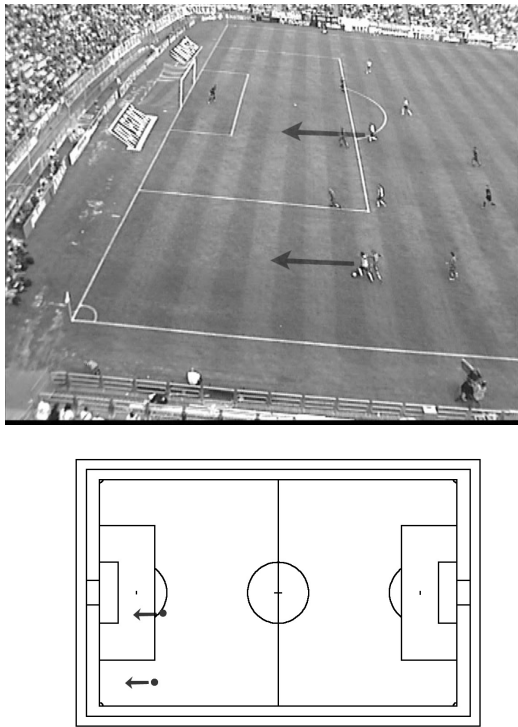


Figure 6: Frame of the video (up) and plane of the football field (down) of the video used. The arrows represent the direction of the players that have been used for the test.

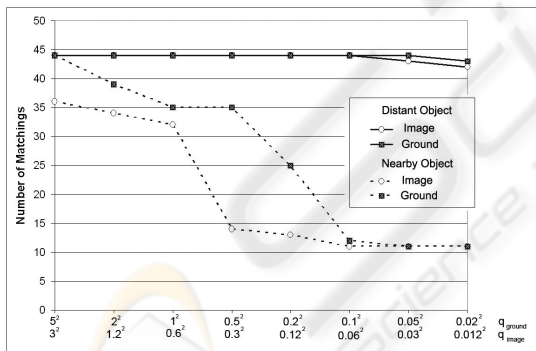


Figure 7: Number of matchings for different state noises. The two scales are equivalent for the position of the distant player.

5 CONCLUSIONS

In this paper we compared a tracker on the image versus a tracker on the ground. A plane projective transformation allows to make the tracking in real coordinates which facilitates the tuning of the tracker, gives measures in real coordinates and allows to relate different cameras in a common reference system. Experimental results from laboratory test and from

real environments proved empirically that the tracker on the ground achieves better results. We have also shown some preliminary results for the automatic recalibration of the camera which avoids some of the practical limitations of the approach. The continuation of this work will be focused to the usage of multiple cameras, having the plane of the surroundings as a common reference for the tracking.

ACKNOWLEDGEMENTS

This work was supported by project OTRI 2005/0388 "UZ - Real Zaragoza - DGA Collaboration Agreement for development of a research project in the sport performance improvement based on the image analysis", and it establishes the grounding for taking real measures and statistics over the ground.

REFERENCES

- A. Criminisi, I. R. and Zisserman, A. (September 1997). A plane measuring device. In *IEEE Transactions on Pattern Analysis and Machine In Proc. BMVC, UK*.
- Bar-Shalom, T. and Fortmann, T. (1988). *Tracking and Data Association*. Academic Press In.
- Durucan, E. and Ebrahimi, T. (October 2001). Change detection and background extraction by linear algebra. In *Proceedings of the IEEE, 89(10):1368-1381*.
- Fabrice Moscheni, S. B. and Kunt, M. (September 1998). Spatiotemporal segmentation based on region merging. In *IEEE Transactions on Pattern Analysis and Machine Intelligence, 20(9):897-915*.
- Guerrero, J. and Sagüés, C. (2003). Robust line matching and estimate of homographies simultaneously. In *IbPRIA, Pattern Recognition and Image Analysis, LNCS 2652, 297-307*.
- Hartley, R. (1997). In defense of the eight-point algorithm. In *IEEE Trans. on Pattern Analysis and Machine Intelligence, 19(6):580-593*.
- Hartley, R. and Zisserman, A. (2000). *Multiple View Geometry in Computer Vision*. Cambridge University Press, Cambridge.
- Herrero, E., Orrite, C., and Senar, J. (2003). Detected motion classification with a double-background and a neighborhood-based difference. In *Pattern Recognition Letters, 24:2079-2092*.
- Isler, V., Khanna, S., Spletzer, J., and Taylor, C. J. (2005). Target tracking with distributed sensors: The focus of attention problem. In *Computer Vision and Image Understanding, 100, 225-247*.
- Kalman, R. E. (1960). New approach to linear filtering and prediction problems. In *Transactions of the ASME—Journal of Basic Engineering, Volume 82, Series D, 35-45*.

- Lee, L., Romano, R., and Stein, G. (August 2000). Monitoring activities from multiple video streams: Establishing a common coordinate frame. In *IEEE Transactions on Pattern Analysis and Machine Intelligence*, 22, n. 8.
- Mundy, J. and Zisserman, A. (1992). *Geometric Invariance in Computer Vision*. MIT Press, Boston.
- Rousseeuw, P. and Leroy, A. (1987). *Robust Regression and Outlier Detection*. John Wiley, New York.
- Tissainayagam, P. and Suter, D. (2001). Visual tracking with automatic motion model switching. In *Pattern Recognition*, 34, 641-660.



SciTeP Press
Science and Technology Publications